EPJ Web of Conferences **274**, 06002 (2022) https://doi.org/10.1051/epjconf/202227406002
XV^{th} Quark Confinement and the Hadron Spectrum

Searching for a leptophobic B boson through $\eta \to \pi^0\gamma\gamma$ and $\eta' \to \pi^0\gamma\gamma$ decays

Rafel Escribano[1,2,*], *Sergi* Gonzàlez-Solís[3,**], and *Emilio* Royo[1,2,***]

[1]Grup de Física Teòrica, Departament de Física, Universitat Autònoma de Barcelona, 08193 Bellaterra (Barcelona), Spain
[2]Institut de Física d'Altes Energies (IFAE) and The Barcelona Institute of Science and Technology, Campus UAB, 08193 Bellaterra (Barcelona), Spain
[3]Theoretical Division, Los Alamos National Laboratory, Los Alamos, NM 87545, USA

Abstract. The sensitivity of the decays $\eta \to \pi^0\gamma\gamma$ and $\eta' \to \pi^0\gamma\gamma$ to a leptophobic B boson in the sub-GeV mass range is summarised in this work. By adding an explicit B-boson resonance exchange to the dominant Standard Model contribution from vector meson exchanges, and employing experimental measurements of the associated branching ratios, the current constraints on the B-boson mass m_B and coupling to Standard Model particles α_B are significantly improved. From these constraints and the analysis of the available experimental $\gamma\gamma$ invariant mass distribution of $\eta \to \pi^0\gamma\gamma$, we conclude that a B-boson signature in the resonant mass range $m_{\pi^0} \lesssim m_B \lesssim m_\eta$ is strongly suppressed and would be very difficult to experimentally identified. The $\eta' \to \pi^0\gamma\gamma$ decay is not as powerful as the $\eta \to \pi^0\gamma\gamma$ at constraining B-boson parameters below m_η but allow exploring larger B-boson masses. Yet, the task of identifying a B-boson with $m_B \sim m_\omega$ would be very challenging.

1 Introduction

An increasingly ubiquitous strategy to search for new physics beyond the Standard Model (BSM) is to test fundamental symmetries in different processes. Decays of the pseudoscalar mesons η and η' are particularly suited to achieve this goal [1, 2]. Examples of this are the rare $\eta^{(\prime)} \to \pi^0\gamma\gamma$ decays which, as they are highly suppressed in the Standard Model (SM) [3], have been put forward as fine probes to search for sub-GeV signatures of a new leptophobic B boson [4] arising from a new $U(1)_B$ gauge symmetry which couples predominantly to quarks over leptons [5].

Experimental searches for leptophobic B bosons depend on the mass m_B and the associated decay channels, and have placed constraints on the coupling for masses that span from below the MeV scale, obtained from long-range nuclear forces and low-energy neutron scattering, to above the GeV scale, obtained at high-energy hadron colliders in dijet resonance searches, as well as in heavy quarkonia and Z decays (see Ref. [1] for an extensive literature related to all these experiments). The intermediate MeV–GeV mass range has been less

*e-mail: rescriba@ifae.es
**e-mail: sergig@lanl.gov
***e-mail: eroyo@ifae.es

© The Authors, published by EDP Sciences. This is an open access article distributed under the terms of the Creative Commons Attribution License 4.0 (http://creativecommons.org/licenses/by/4.0/).

explored thus far [4, 5], which is down to this being the region of non-perturbative QCD, and has often been considered as a challenging blindspot for experiment in the past. However, searches for leptophobic B bosons are gaining traction in this intermediate mass range given the potential signatures that can be looked for in decays of light mesons, such as η, η', ω, and ϕ [4], after years of sterile sub-GeV dark-photon searches most of them relying on the coupling of this new force to leptons in decays to e^+e^- and $\mu^+\mu^-$ pairs [1]. In fact, the search for leptophobic B bosons has been incorporated into the physics programmes of existing light-meson collaborations such as KLOE-II, which is searching for B bosons by looking for enhancements in the $\pi^0\gamma$ invariant mass spectrum of the $\phi \to \eta B \to \eta\pi^0\gamma$ process [6], and is a top priority physics goal for the recently approved Jefferson Lab Eta Factory (JEF) experiment, which promises a new and exciting era for η and η' physics, with the $\eta \to \pi^0\gamma\gamma$ decay being their key signal channel. B-boson searches may also be carried out at future η/η' facilities, such as the proposed REDTOP experiment [2].

The model that we consider in this work for a $U(1)_B$ leptophobic gauge boson B that couples to the baryon number has the following interaction Lagrangian [4, 5]

$$\mathcal{L}_{\text{int}} = \left(\frac{1}{3}g_B + \varepsilon Q_q e\right)\bar{q}\gamma^\mu q B_\mu - \varepsilon e \bar{\ell}\gamma^\mu \ell B_\mu \,, \tag{1}$$

where B_μ is the new gauge boson field and g_B is the new gauge coupling, with $\alpha_B = g_B^2/4\pi$ being the fine structure constant associated to the baryonic force. This interaction structure is gauge invariant and preserves the low-energy symmetries of QCD.

Partial widths for B-boson decays in the MeV–GeV mass range have been calculated in [4] using the hidden local symmetry framework for vector meson dominance (VMD). Above the single-pion threshold, $m_{\pi^0} \lesssim m_B \lesssim 1$ GeV, the B boson decays predominantly to $\pi^0\gamma$, or to $\pi^0\pi^+\pi^-$ when kinematically allowed, very much like the ω meson. In fact, the B boson can be assigned the same quantum numbers as those from the ω, *i.e.* $I^G(J^{PC}) = 0^-(1^{--})$. It must be noted that the interaction Lagrangian in Eq. (1) is not completely decoupled from leptons as it contains subleading photon-like couplings to leptons proportional to $\varepsilon = eg_B/(4\pi)^2$.

At present, conservative constraints from η and η' decays on the B-boson parameters α_B and m_B are based on total rates setting the SM contribution to zero and making use of the narrow width approximation (NWA) [4]. It must be stressed, though, that the SM contribution to these decays is not negligible [3] and, therefore, it should not be disregarded in exclusion analyses of B bosons. Thus, one of the goals of the work presented in [7] is to take into account SM effects in these analyses. To that effect, we employ our controlled SM contributions from Ref. [3], we supplement it with the explicit inclusion of an intermediate B boson and use the most up-to-date experimental data.

Significantly greater sensitivity to the B-boson model could be obtained from the analysis of the invariant mass distributions. Provided that $m_{\pi^0} \leq m_B \leq m_{\eta^{(\prime)}}$, the B-boson mediated decay $\eta^{(\prime)} \to B\gamma \to \pi^0\gamma\gamma$ would reveal a peak at around m_B in the $\pi^0\gamma$ invariant mass spectrum. Searches for a $\pi^0\gamma$ resonance within this mass region in $\eta \to \pi^0\gamma\gamma$ decays are the main physics goal of the JEF experiment, which plans to improve the total rate limit by two orders of magnitude, and is being searched for by KLOE-II via $\phi \to \eta B \to \eta\pi^0\gamma$ [6] and $\eta \to B\gamma \to \pi^0\gamma\gamma$. Accordingly, we aim to perform a detailed analysis of the $\gamma\gamma$ and $\pi^0\gamma$ invariant mass distributions. In particular, using the available experimental diphoton spectra, together with our SM and B-boson amplitudes, we determine which regions of the α_B–m_B plane are preferred by the data and assess the B-boson contribution. Searches for leptophobic B bosons require experimental precision, in order to disentangle their contribution from the SM, but also robust theoretical predictions.

2 Theoretical Framework

2.1 Standard Model: dominant vector contributions

VMD can be used to calculate the dominant SM contributions from vector meson resonance exchanges to the $\eta^{(\prime)} \to \pi^0\gamma\gamma$ decay processes. In the VMD picture, the decay $\eta^{(\prime)} \to \pi^0\gamma\gamma$ proceeds through the transition $\eta^{(\prime)} \to V\gamma$ followed by $V \to \pi^0\gamma$, resulting in a total of six diagrams contributing to the amplitude of the process, which corresponds to the exchange of the three neutral vector mesons $V = \rho^0, \omega$ and ϕ in the t and u channels. By combining the $V\eta^{(\prime)}\gamma$ and $V\pi^0\gamma$ interacting terms with the propagator of the exchanged vector mesons, one can calculate the vector meson contributions to the $\eta^{(\prime)} \to \pi^0\gamma\gamma$ decays. We found [3]

$$\mathcal{A}^{\mathrm{VMD}}_{\eta^{(\prime)}\to\pi^0\gamma\gamma} = \sum_{V=\rho^0,\omega,\phi} g_{V\eta^{(\prime)}\gamma} g_{V\pi^0\gamma} \left[\frac{(P\cdot q_2 - m^2_{\eta^{(\prime)}})\{a\} - \{b\}}{D_V(t)} + \left\{ \begin{array}{c} q_2 \leftrightarrow q_1 \\ t \leftrightarrow u \end{array} \right\} \right] , \tag{2}$$

where $t, u = (P - q_{2,1})^2 = m^2_\eta - 2P\cdot q_{2,1}$ are Mandelstam variables, $\{a\}$ and $\{b\}$ are the Lorentz structures defined as

$$\begin{aligned} \{a\} &= (\epsilon_1\cdot\epsilon_2)(q_1\cdot q_2) - (\epsilon_1\cdot q_2)(\epsilon_2\cdot q_1) , \\ \{b\} &= (\epsilon_1\cdot q_2)(\epsilon_2\cdot P)(P\cdot q_1) + (\epsilon_2\cdot q_1)(\epsilon_1\cdot P)(P\cdot q_2) \\ &\quad - (\epsilon_1\cdot\epsilon_2)(P\cdot q_1)(P\cdot q_2) - (\epsilon_1\cdot P)(\epsilon_2\cdot P)(q_1\cdot q_2) , \end{aligned} \tag{3}$$

where P is the four-momentum of the decaying η meson, and $\epsilon_{1,2}$ and $q_{1,2}$ are the polarisation and four-momentum vectors of the final photons, respectively. The denominator $D_V(q^2) = m^2_V - q^2 - i\, m_V\Gamma_V$ is the vector meson propagator, with $V = \rho^0$, ω and ϕ. Due to the fact the the ρ^0 meson has got a very large decay width, the use of the usual Breit-Wigner prescription is not justified and, thus, one is compelled to make use of an energy-dependent decay width

$$\Gamma_{\rho^0}(q^2) = \Gamma_{\rho^0} \left(\frac{q^2 - 4m^2_\pi}{m^2_{\rho^0} - 4m^2_\pi} \right)^{3/2} \theta(q^2 - 4m^2_\pi) . \tag{4}$$

For our analysis, we fix the $g_{VP\gamma}$ couplings in Eq. (2) from the comparison of the calculated decay widths for the radiative transitions $V \to P\gamma$ and $P \to V\gamma$ with their empirical values from the PDG [8].

2.2 Beyond the Standard Model: B-boson contribution

In analogy to the VMD contributions summarised in the previous subsection, we next define the framework to include intermediate B-boson exchanges to the decay amplitude. This contribution can be assessed from the conventional VMD VVP and $V\gamma$ Lagrangians [9] supplemented by an effective Lagrangian that describes the VB interaction. The latter is formally identical to the $V\gamma$ Lagrangian with the substitutions $A^\mu \to B^\mu$, $e \to g_B$ and $Q \to \mathrm{diag}\{1/3, 1/3, 1/3\}$. From the VVP and VB Lagrangians along with the corresponding V-meson propagators, it is straightforward to obtain expressions for the $g_{BP\gamma}$ couplings in terms of the generic B-boson coupling g_B. The $g_{BP\gamma}$ couplings are energy dependent and read

$$\begin{aligned} g_{B\pi^0\gamma}(q^2) &= \frac{e g_B}{4\pi^2 f_\pi} F_\omega(q^2) , \\ g_{B\eta\gamma}(q^2) &= \frac{e g_B}{12\pi^2 f_\pi} \left[\mathrm{c}\varphi_P F_\omega(q^2) + \sqrt{2}\mathrm{s}\varphi_P F_\phi(q^2) \right] , \\ g_{B\eta'\gamma}(q^2) &= \frac{e g_B}{12\pi^2 f_\pi} \left[\mathrm{s}\varphi_P F_\omega(q^2) - \sqrt{2}\mathrm{c}\varphi_P F_\phi(q^2) \right] , \end{aligned} \tag{5}$$

where φ_P is the η-η' mixing angle in the quark-flavour basis [10] and the abbreviations $c\varphi_P \equiv \cos\varphi_P$ and $s\varphi_P \equiv \sin\varphi_P$ have been employed. The functions $F_V(q^2)$ in the previous equations are form factors that account for the ω and ϕ propagation, and are given by $F_V(q^2) = m_V^2/(m_V^2 - q^2 - im_V\Gamma_V)$.

Combining the $g_{B\pi^0\gamma}$ and $g_{B\eta^{(\prime)}\gamma}$ couplings from Eq. (5) with the propagator of the B boson, allows one to find the B-boson exchange contribution to the amplitude of the $\eta^{(\prime)} \to \pi^0\gamma\gamma$ decays

$$\mathcal{A}^{B\,\text{boson}}_{\eta^{(\prime)}\to\pi^0\gamma\gamma} = g_{B\eta^{(\prime)}\gamma}(t)g_{B\pi^0\gamma}(t)\left[\frac{(P\cdot q_2 - m^2_{\eta^{(\prime)}})\{a\} - \{b\}}{D_B(t)} + \left\{\begin{array}{c} q_2 \leftrightarrow q_1 \\ t \leftrightarrow u \end{array}\right\}\right], \tag{6}$$

where $D_B(q^2) = m_B^2 - q^2 - im_B\Gamma_B$ is the B-boson propagator.

The decay widths for the radiative transitions $\eta^{(\prime)} \to B\gamma$ and $B \to \pi^0\gamma, \eta^{(\prime)}\gamma$ can be calculated from Eq. (5) and are given in [7]. The leptonic decays, which arise from the kinetic mixing of the B boson with the photon, cf. Eq. (1), and the B-boson decay to $\pi^+\pi^-$, which also depends on ϵ, are given in [4]

3 Limits on α_B and m_B

In this section, we make use of the theoretical expressions presented in Secs. 2.1 and 2.2, along with the available experimental data, to place limits on the B-boson parameters α_B and m_B.

The corresponding partial decay widths of the $\eta^{(\prime)} \to \pi^0\gamma\gamma$ processes depend on a total of three parameters: i) the baryonic fine-structure constant, α_B, ii) the B-boson mass, m_B, and iii) its total decay width, Γ_B. However, given that Γ_B is not an independent parameter (that is, it can be expressed in terms of α_B and m_B), we can reduce the number of free parameters from three to two. Accordingly, the denominator in Eq. (6), $D_B(q^2)$, is replaced by $\mathcal{D}_B(q^2) = m_B^2 - q^2 - i\sqrt{q^2}\,\Gamma_B(q^2)$, where $\Gamma_B(q^2) = \sum_i \Gamma_B^i(q^2)$ is the energy-dependent width of the B boson, with the sum running over the partial widths of the various decay channels the B boson can decay into. For our study, we include the partial widths of the decay channels $B \to \pi^0\gamma$, e^+e^-, $\mu^+\mu^-$, $\pi^+\pi^-$, and $\pi^0\pi^+\pi^-$.

Next, we proceed to calculate the constraints on the B-boson parameters α_B and m_B set by experiment. We start with the $\eta \to \pi^0\gamma\gamma$ decay using the PDG reported value, BR = $(2.56 \pm 0.22) \times 10^{-4}$ [8], as well as the (preliminary) value from the KLOE collaboration, BR = $(1.23 \pm 0.14) \times 10^{-4}$ [6]. In Fig. 1, we show the limits in the α_B–m_B plane, which are found by requiring our predictions to not exceed the corresponding branching ratios at 2σ. The grey area is excluded by the data from KLOE, which yield a more stringent limit than the resulting one from the PDG (solid red line). This is as expected given that the BR from KLOE is found to be in good agreement with our SM prediction from Ref. [3], BR = $(1.35 \pm 0.08) \times 10^{-4}$, and, thus, the KLOE constraints on the B boson turn out to be stronger. The dashed black line in the figure is found using the data from KLOE but with the SM (or, equivalently, QCD) contributions set to zero. Clearly, these contributions are not negligible as the limits on α_B become an order of magnitude weaker when their effects are turned off (labelled QCD off in the plots).

The shape and size of the excluded region in Fig. 1 contains key physical information. In this figure, three different regions are observed. The first one corresponds to $m_B \lesssim m_{\pi^0}$, where $\alpha_B \sim \mathcal{O}(1)$. At $m_B \sim m_{\pi^0}$, the limit placed on the coupling plummets by almost six orders of magnitude down to $\alpha_B \sim 10^{-6}$; it then moderately increases, to finally take a steep rise when m_B approaches m_η, reaching $\alpha_B \sim 10^{-2}$. Finally, for $m_B \gtrsim m_\eta$ the constraint on the coupling

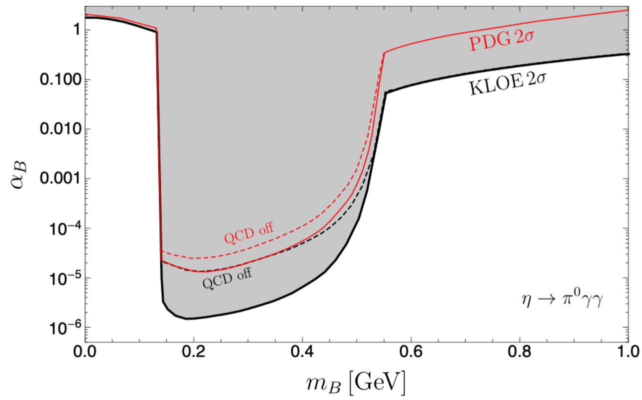

Figure 1. Limits on the leptophobic B-boson coupling α_B for different m_B masses from the $\eta \to \pi^0\gamma\gamma$ BR measurements by KLOE [6] (black line) and the PDG [8] (red line). The grey shaded region is excluded by KLOE and the dashed lines correspond to the limits with the QCD contributions turned off.

grows very smoothly as m_B increases. Out of the three, the $m_{\pi^0} \lesssim m_B \lesssim m_\eta$ region deserves special attention and raises the question as to why α_B is constrained so strongly there. The answer to this is related to the fact that the B-boson width is extremely small in this region of parameter space.

Next, we show the exclusion plot associated to the $\eta' \to \pi^0\gamma\gamma$ decay in Fig. 2, where we display the region of the α_B–m_B plane excluded by the BESIII collaboration measurement, BR $= (3.20 \pm 0.07 \pm 0.23) \times 10^{-3}$ [11], at a confidence level of 2σ. The shape of the excluded region for the $\eta' \to \pi^0\gamma\gamma$ is clearly different to that of the $\eta \to \pi^0\gamma\gamma$ decay (cf. Fig. 1). In particular, the limits within the $m_{\pi^0} \lesssim m_B \lesssim m_\eta$ mass range, whilst still showing the shape resembling a keel, are about 4 orders of magnitude weaker than those coming from $\eta \to \pi^0\gamma\gamma$.

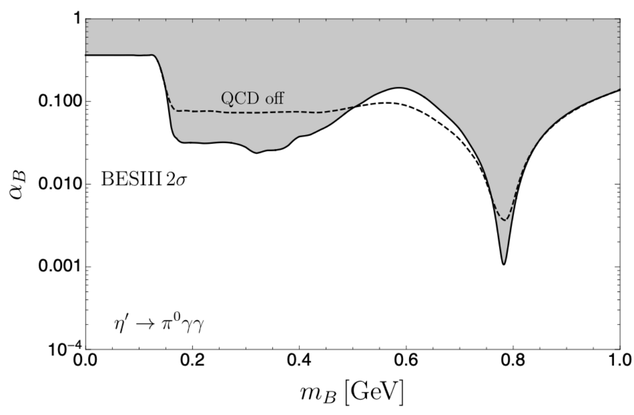

Figure 2. Limits on the leptophobic B-boson coupling α_B for different m_B masses from the BR measurements of the decay $\eta' \to \pi^0\gamma\gamma$ [11] by BESIII. The grey shaded region is excluded and the dashed black line corresponds to the limit with the QCD contributions set to zero.

All in all, the $\eta' \to \pi^0\gamma\gamma$ decay does not appear to be as powerful as the $\eta \to \pi^0\gamma\gamma$ for constraining the B-boson parameters.

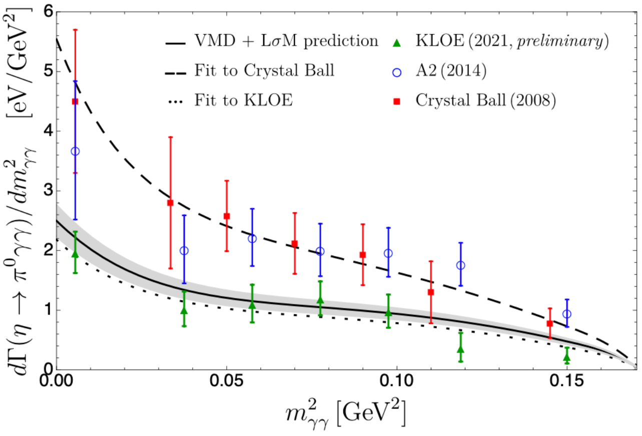

Figure 3. KLOE (green triangles), A2 (blue circles) [12] and Crystal Ball (red squares) [13] measurements of the $m^2_{\gamma\gamma}$ spectrum for the $\eta \to \pi^0\gamma\gamma$ decay, as well as the SM prediction [3] (solid black line) and SM with B-boson predictions using the fitted parameters from Eqs. (7) and (8).

Let us now move on to perform statistical fits to the available experimental diphoton spectra to determine the region of the α_B–m_B plane (cf. Fig. 1) that is preferred by the data. From the Crystal Ball $\gamma\gamma$ invariant mass spectrum [13], we obtain the following best fit values

$$\alpha_B = 0.40^{+0.07}_{-0.08}\,, \quad m_B = 583^{+32}_{-20}\ \text{MeV}\,, \tag{7}$$

with a $\chi^2_{\text{min}}/\text{d.o.f} = 0.42/5 = 0.08$, whereas, for the KLOE (preliminary) data[1], we find

$$\alpha_B = 0.049^{+40}_{-27}\,, \quad m_B = 135^{+1}_{-135}\ \text{MeV}\,, \tag{8}$$

with a $\chi^2_{\text{min}}/\text{d.o.f} = 4.46/5 = 0.89$. Because of the large errors associated to the experimental points from Crystal Ball, its $\chi^2_{\text{min}}/\text{d.o.f}$ turns out to be extremely small. The $\chi^2_{\text{min}}/\text{d.o.f}$ of the fit to the KLOE data implies a good quality of the fit. The errors associated to the fitted parameters have been estimated by perturbing one of the parameters at a time such that $\chi^2 = \chi^2_{\text{min}} + 1$ [8]. The theoretical $\gamma\gamma$ invariant mass spectra using the parameters from the fits in Eqs. (7) and (8) to the Crystal Ball and KLOE data are shown in Fig. 3 with dashed and dotted black lines, respectively. Also plotted are the experimental data points and the SM prediction [3] (solid black line) with an estimation of the uncertainty from the error propagation of the $VP\gamma$ couplings. It is worth noticing that the inclusion of a non-resonant B boson in the t and u channels, with parameters from Eq. (7), helps explain the tension between the Crystal Ball spectrum and the SM result [3]. Notwithstanding this, the best fit parameters from Crystal Ball in Eq. (7) are ruled out by the KLOE data (cf. Fig. 1), whose measured BR continues the decreasing trend seen over the decades associated to more precise measurements becoming available. In turn, this trend supports the theoretical treatment without a B boson, as our VMD approach from Ref. [3] appears to be capable of successfully predicting the experimental data

[1]Whilst KLOE has published a BR for the $\eta \to \pi^0\gamma\gamma$ process in a conference proceedings [6], the diphoton spectrum has not yet been published, although it was presented at The 10$^{\text{th}}$ International Workshop on Chiral Dynamics 2021. For our analysis, we have retrieved the data points from their presentation's figure

for the two $\eta^{(\prime)} \to \pi^0\gamma\gamma$ decays simultaneously. Clearly, the experimental situation is far from conclusive and it may not be possible to make categorical statements about the need for a B boson until the arrival of new and more precise data, *e.g.* from the KLOE(-II) and JEF experiments.

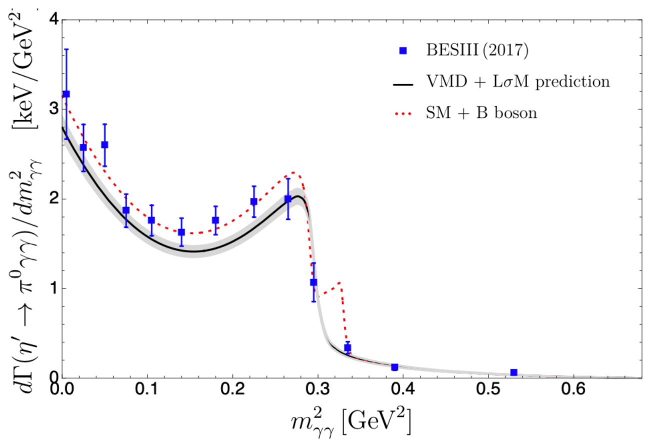

Figure 4. BESIII (blue squares) [11] measurements of the $m^2_{\gamma\gamma}$ spectrum for the $\eta' \to \pi^0\gamma\gamma$ decay, as well as the SM prediction [3] (solid black line) and SM with B-boson prediction using the fitted parameters from Eq. (9) (dotted red line).

Next, we perform fits to the $\eta' \to \pi^0\gamma\gamma$ diphoton spectrum from the BESIII collaboration [11], which may be used to explore larger B-boson masses. The fit to the $\eta' \to \pi^0\gamma\gamma$ data yields

$$\alpha_B = 0.005(1)\,, \quad m_B = 759(1)\ \text{MeV}\,, \tag{9}$$

with $\chi^2_{\text{min}}/\text{d.o.f} = 11.73/11 = 1.07$. The distribution using the fitted parameters from Eq. (9) is shown in Fig. 4 (dotted red line), together with the experimental data (blue squares) and the SM prediction [3] (solid black line) with an estimation of its uncertainty. It is worth noticing the sudden drop in the dotted red line (*i.e.* SM with B-boson distribution) at $m^2_{\gamma\gamma} \approx 0.33$ GeV^2. What is interesting about this is that, even though the $\chi^2_{\text{min}}/\text{d.o.f}$ of this fit is very good, the associated integrated branching ratio deviate from the experimental counterpart due to the effect of the wiggle on the distribution. Also, the spectrum using the fit parameters would lead to larger than observed bin values for the experimental points 10 and 11.

To conclude, it is worth highlighting that both our SM and SM with B-boson predictions agree well with both sets of experimental data points. The largest differences between the theoretical predictions still show compatibility at roughly the 1σ level. We, therefore, conclude that the experimental data from KLOE and BESIII for the $\eta \to \pi^0\gamma\gamma$ and $\eta' \to \pi^0\gamma\gamma$ decays, respectively, do not require a B-boson contribution, in spite of the coupling α_B being clearly non-zero.

4 Conclusions

The sensitivity of the decays $\eta \to \pi^0\gamma\gamma$ and $\eta' \to \pi^0\gamma\gamma$ to a leptophobic B boson in the sub-GeV mass range is summarised in this work. Adding the explicit B-boson exchange contribution to the SM amplitude dominated by the exchange of the lightest vector resonances within a VMD framework, has allowed us to place stringent limits on the B-boson parameters

m_B and α_B by comparing with current experimental data. From the analysis of the $\eta \to \pi^0\gamma\gamma$, we have strengthened by one order of magnitude the current constraints in the resonant mass region $m_{\pi^0} \lesssim m_B \lesssim m_\eta$, reaching $\alpha_B \sim 10^{-6}$. These constraints would make a B-boson signature strongly suppressed, rendering the task of experimentally identifying it as a peak around m_B in the $\pi^0\gamma$ invariant mass distribution practically impossible. Our analysis of the most recent experimental $\gamma\gamma$ invariant mass distribution from the KLOE collaboration supports the description of the processes studied in this work without contribution from a potential new leptophobic B boson, as our SM treatment is capable of simultaneously predicting the two $\eta^{(\prime)} \to \pi^0\gamma\gamma$ decays with remarkable agreement with the experimental data. Finally, the $\eta' \to \pi^0\gamma\gamma$ decay is not as powerful as the $\eta \to \pi^0\gamma\gamma$ at constraining B-boson parameters.

Acknowledgements

R. E. would like to express his gratitude to the QCHS22 Organising Committee for the opportunity of presenting this contribution, and for the pleasant and interesting conference we have enjoyed.

The work of S. G-S. is supported by the Laboratory Directed Research and Development program of Los Alamos National Laboratory under project number 20210944PRD2, and by the U.S. Department of Energy through the Los Alamos National Laboratory. Los Alamos National Laboratory is operated by Triad National Security, LLC, for the National Nuclear Security Administration of U.S. Department of Energy (Contract No. 89233218CNA000001). The work of R. E. and E. R. has been supported by the Spanish Ministry of Science and Innovation under project number PID2020-112965GB-I00, and by the European Union's Horizon 2020 Research and Innovation Programme under grant no. 824093 (H2020- INFRAIA-2018-1). IFAE is partially funded by the CERCA program of the Generalitat de Catalunya.

References

[1] L. Gan, B. Kubis, E. Passemar, S. Tulin, Phys. Rept. **945**, 1 (2022), `2007.00664`
[2] J. Elam et al. (REDTOP) (2022), `2203.07651`
[3] R. Escribano, S. Gonzàlez-Solís, R. Jora, E. Royo, Phys. Rev. D **102**, 034026 (2020), `1812.08454`
[4] S. Tulin, Phys. Rev. D **89**, 114008 (2014), `1404.4370`
[5] A.E. Nelson, N. Tetradis, Phys. Lett. B **221**, 80 (1989)
[6] B. Cao (KLOE-2), PoS **EPS-HEP2021**, 409 (2022)
[7] R. Escribano, S. Gonzàlez-Solís, E. Royo (2022), `2207.14263`
[8] P.A. Zyla et al. (Particle Data Group), PTEP **2020**, 083C01 (2020)
[9] A. Bramon, A. Grau, G. Pancheri, Phys. Lett. B **283**, 416 (1992)
[10] A. Bramon, R. Escribano, M.D. Scadron, Eur. Phys. J. C **7**, 271 (1999), `hep-ph/9711229`
[11] M. Ablikim et al. (BESIII), Phys. Rev. D **96**, 012005 (2017), `1612.05721`
[12] B.M.K. Nefkens et al. (A2 at MAMI), Phys. Rev. C **90**, 025206 (2014), `1405.4904`
[13] S. Prakhov et al., Phys. Rev. C **78**, 015206 (2008)